LETTER

doi:10.1038/nature13722

Epigenetic reprogramming that prevents transgenerational inheritance of the vernalized state

Pedro Crevillén[1]†, Hongchun Yang[1], Xia Cui[2], Christiaan Greeff[1]†, Martin Trick[1], Qi Qiu[2], Xiaofeng Cao[2] & Caroline Dean[1]

The reprogramming of epigenetic states in gametes and embryos is essential for correct development in plants and mammals[1]. In plants, the germ line arises from somatic tissues of the flower, necessitating the erasure of chromatin modifications that have accumulated at specific loci during development or in response to external stimuli. If this process occurs inefficiently, it can lead to epigenetic states being inherited from one generation to the next[2–4]. However, in most cases, accumulated epigenetic modifications are efficiently erased before the next generation. An important example of epigenetic reprogramming in plants is the resetting of the expression of the floral repressor locus *FLC* in *Arabidopsis thaliana*. *FLC* is epigenetically silenced by prolonged cold in a process called vernalization. However, the locus is reactivated before the completion of seed development, ensuring the requirement for vernalization in every generation. In contrast to our detailed understanding of the polycomb-mediated epigenetic silencing induced by vernalization, little is known about the mechanism involved in the reactivation of *FLC*. Here we show that a hypomorphic mutation in the jumonji-domain-containing protein ELF6 impaired the reactivation of *FLC* in reproductive tissues, leading to the inheritance of a partially vernalized state. ELF6 has H3K27me3 demethylase activity, and the mutation reduced this enzymatic activity *in planta*. Consistent with this, in the next generation of mutant plants, H3K27me3 levels at the *FLC* locus stayed higher, and *FLC* expression remained lower, than in the wild type. Our data reveal an ancient role for H3K27 demethylation in the reprogramming of epigenetic states in plant and mammalian embryos[5–7].

Many *A. thaliana* accessions overwinter before flowering, as a result of FRIGIDA (FRI)-mediated high-level expression of a floral repressor called FLC[8,9]. Prolonged cold during the weeks of winter antagonizes this activation and progressively epigenetically silences *FLC*. This process enables other floral promotion signals, such as day length, to induce flowering in spring. The epigenetic silencing of *FLC* involves polycomb-mediated chromatin regulation[10–12] and is maintained until embryogenesis, when *FLC* expression is reset to ensure a requirement for vernalization in every generation[13,14]. The resetting of *FLC* expression occurs in the early globular embryo[13,14]; then, *FLC* expression increases throughout embryo development until it reaches maximum levels when the seed has completely formed[14]. However, the molecular mechanisms underlying *FLC* resetting are unknown, and several factors that are required for the upregulation of *FLC* in vegetative tissues have been shown to be dispensable for *FLC* expression in the embryo[14]. One exception is the yeast SWR1 homologue PIE1 (ref. 14), although it is unclear whether *pie1* mutations are resetting-specific defects because these mutations strongly reduce *FLC* expression across the plant independently of vernalization status.

To dissect this resetting mechanism, we isolated mutants that are defective in the reactivation of *FLC* after vernalization (Extended Data Fig. 1a). The parental line was an *A. thaliana* Landsberg erecta (Ler) plant carrying an *FLC*::luciferase (*FLC*::*LUC*) translational fusion and an active *FRI* transgene[15]. We searched for plants in which *FLC* expression was silenced by vernalization but, unlike in the wild type, was not fully restored in the following generation (Fig. 1a), leading to inheritance of the vernalized state. The frequency of these mutations was low (with only 2 mutants identified from the progeny of 6,000 mutagenized parent lines), in contrast to the more common class of mutations, which involved early flowering before vernalization as a result of reduced *FLC* expression (Extended Data Fig. 1b). The first resetting mutant that was isolated was found to be recessive (Extended Data Fig. 2a) and flowered slightly earlier without vernalization than did the wild type (Fig. 1b). In the generation after vernalization, the mutant flowered even earlier and had significantly

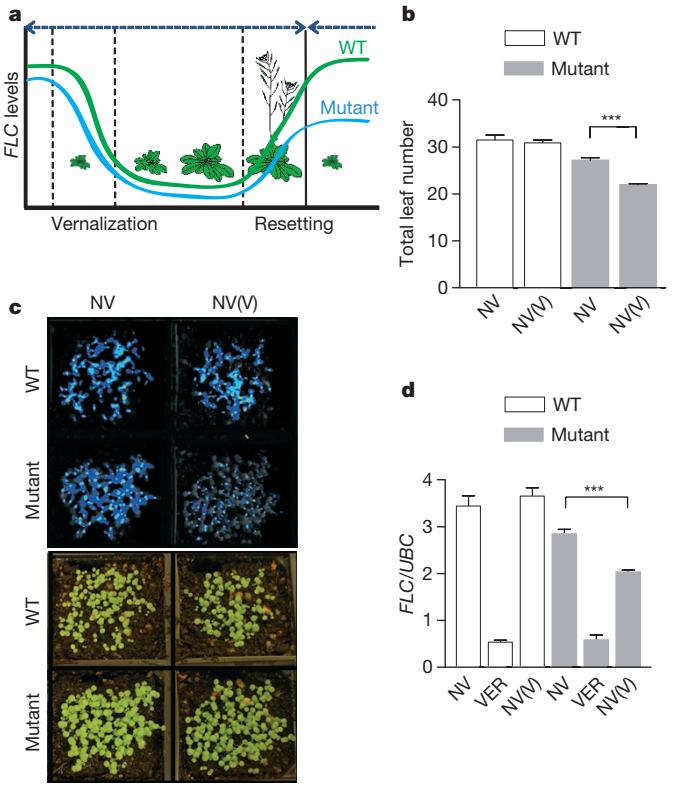

Figure 1 | Isolation and characterization of the resetting mutant. **a**, The rationale for the genetic screen. The parental wild type (WT) is Ler (*FRI*) *FLC*::*LUC*; the mutant is a resetting mutant. **b**–**d**, The resetting mutant is early flowering (**b**), with fewer leaves when bolting (with flowering time assayed as total leaf number), and maintains low *FLC* expression, as shown by *FLC*–luciferase imaging of 8-day-old seedlings (**c**) and by quantitative reverse transcription PCR (qRT–PCR) analysis normalized to *UBC* levels (**d**). Pseudocolour bioluminescent images (**c**, top) from blue (least intense) to red (most intense) and normal images (**c**, bottom) of the same plants are presented. The data are presented as the mean + s.e.m., $n = 20$ (**b**) and $n = 3$ (**d**); $^{***}P < 0.001$. NV, non-vernalized; NV(V), non-vernalized following vernalization in the previous generation; VER, vernalized.

[1]Department of Cell & Developmental Biology, John Innes Centre, Norwich Research Park, Norwich NR4 7UH, UK. [2]State Key Laboratory of Plant Genomics and National Center for Plant Gene Research, Institute of Genetics and Developmental Biology, Chinese Academy of Sciences. Beijing 100101, China. †Present addresses: Centro de Biotecnología y Genómica de Plantas, UPM-INIA, 28223 Madrid, Spain (P.C.); Department of Biology, Copenhagen University, DK-2200 Copenhagen, Denmark (C.G.).

reduced *FLC* expression (Fig. 1c, d), albeit about fourfold higher than in fully vernalized seedlings (Fig. 1d). The resetting mutant therefore causes transgenerational inheritance of a partially vernalized state. The early flowering phenotype was stable for at least three generations following vernalization (Extended Data Fig. 2b) but was not enhanced by a second vernalization treatment in the later generations. No other strong developmental phenotypes were observed.

The mutant phenotype was strongly affected by the segregation of modifiers in a traditional Ler × Columbia (Col) cross, which is normally used for genetic mapping, and the mutation was only narrowed to a ~500 kilobase region on chromosome 5. We therefore sequenced the whole genome of the mutant plant and analysed the linkage of candidate single nucleotide polymorphisms (SNPs) in an F_2 population generated from a cross between the mutant and the isogenic progenitor line. This strategy identified a SNP in *ELF6* (AT5G04240) that co-segregated with the resetting phenotype (Extended Data Fig. 3). To confirm that the resetting phenotype was caused by this mutant allele (named *elf6-5*), we complemented the mutation using the wild-type *ELF6* gene under the control of its own regulatory sequences. Vernalized T_2 transgenic *elf6-5* lines carrying the wild-type *ELF6* transgene showed wild-type *FLC* expression levels in the siliques (Fig. 2a, b). Thus, we concluded that the single nucleotide mutation in *ELF6* causes the mutant phenotype.

ELF6 is a jumonji-C-domain-containing protein that is closely related to the histone H3 trimethylated lysine 27 (H3K27me3) demethylase REF6 (ref. 16), and it is expressed at low levels in seedlings but at high levels in flowers and embryos (Fig. 2c–f). In the *elf6*-5 mutants, an alanine is replaced with a valine (amino acid 424) at the carboxy-terminal end of the jumonji C domain (Fig. 2g). This amino acid is conserved in REF6 and the human H3K27me3 demethylases UTX (also known as KDM6A) and JMJD3 (also known as KDM6B) (Fig. 2g). This high degree of conservation suggests that this residue may be crucial for the function of the protein. A null *elf6* T-DNA insertion allele has been shown to be early flowering because of increased expression of *FT*[17], an integrator gene that promotes floral transition. In addition, we found less *FLC* expression in seedlings carrying this knockout allele (*elf6-3*) than in wild-type Col seedlings (Extended Data Fig. 4a), confirming that ELF6 regulates *FLC* expression. The early flowering phenotype and low *FLC* expression in *elf6-3* seedlings precluded observation of the resetting phenotype (Extended Data Fig. 4b). Although the different genetic backgrounds of the two alleles may complicate interpretation, these data suggest that the alanine-to-valine substitution in *elf6-5* plants confers a hypomorphic phenotype, affecting an activity that is particularly important for resetting *FLC* expression during reproductive development.

Consistent with a role for ELF6 in regulating *FLC* resetting, the *elf6-5* allele had a much larger effect on *FLC* expression in flowers and siliques than in seedlings (Fig. 3a, b). To define more precisely when the *elf6-5* mutant disrupts *FLC* expression, we measured *FLC* messenger RNA levels at different stages of silique development[18], a proxy for *FLC* expression in the embryo[13,14]. Low *FLC* mRNA levels were detected in young siliques from the vernalized parental line (SQ16 and SQ17a) (Fig. 3c), and these levels increased as the silique matured (SQ17b1 and SQ17b2), reaching a maximum when the silique started to desiccate and the embryo became fully developed (SQ18). In the vernalized resetting mutant, *FLC* mRNA was detected in young, developing siliques, but it was not upregulated to wild-type levels at the later stages (Fig. 3c). Comparison of siblings differing only by an *FLC*::*GUS* (β-glucuronidase) reporter[19] showed that *FLC*::*GUS* expression was lower in the early globular embryo of *elf6-5* mutants than in the wild type (Fig. 3d). This finding suggests that ELF6 increases *FLC* expression as the embryo develops. There may be no clear mechanistic separation between reprogramming the epigenetic state and setting the *FLC* expression level.

The *FLC* locus has a complex transcriptional circuitry, including a set of antisense transcripts called *COOLAIR* that are induced during vernalization but are also expressed in the warm[20]. We wondered whether the *elf6-5* resetting mutant also affected *COOLAIR* expression. Surprisingly, no difference between the mutant and the wild type was found, and *COOLAIR* transcripts were upregulated normally in the mutant in developing siliques (Fig. 3e). Therefore, in contrast to mutants in which both *FLC* sense and total *COOLAIR* expression levels change coordinately (for example, *fri* mutants), the mutation in *elf6-5* plants uncouples *FLC* sense and antisense regulation.

Many other loci are epigenetically modified during *A. thaliana* gamete formation and embryo development[21,22]. We tested whether the *elf6-5* allele influences transposon expression, by analysing specific short interfering

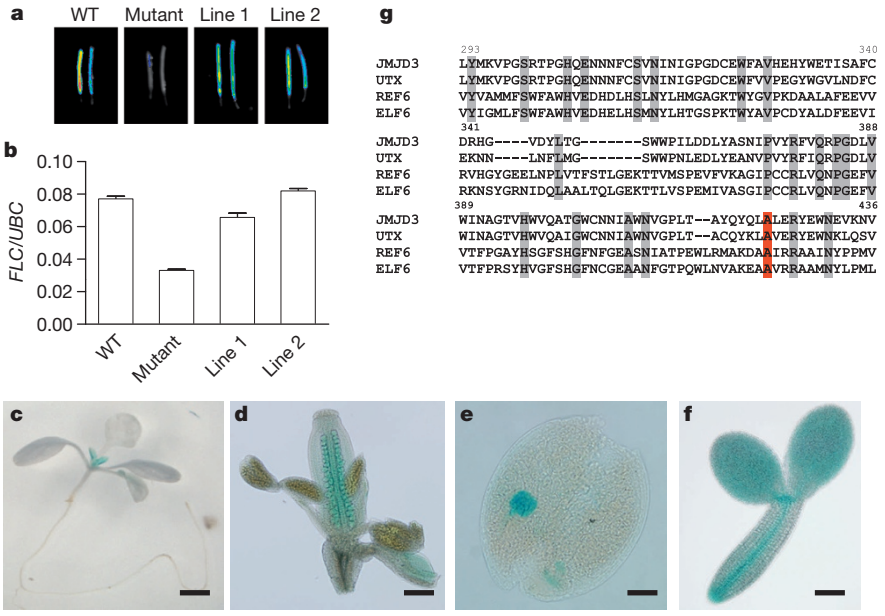

Figure 2 | Mapping of the resetting mutant. **a**, **b**, An *ELF6* genomic construct complements the resetting mutant. *FLC*–luciferase imaging (**a**) and *FLC* qRT–PCR data (**b**) from mature siliques from the vernalized WT, the *elf6-5* mutant and representative T_2 *elf6-5* (*pELF6*::*ELF6*) lines (Line1 and Line2). Pseudocolour bioluminescent image (**a**) from blue (least intense) to red (most intense). **c**–**f**, *ELF6*::*GUS* (blue) expression profile in a 7-day-old seedling (**c**), ovules (**d**), a globular embryo (**e**) and a mature embryo (**f**). Scale bars, 5 mm (**c**), 250 μm (**d**), 50 μm (**e**, **f**). **g**, The ELF6 amino acid residue that is mutated in *elf6-5* mutants is conserved (red; A, alanine). A sequence alignment of the jumonji C domain of *A. thaliana* ELF6 and REF6 and human JMJD3 and UTX proteins is shown. Highly conserved residues are shaded in grey. The numbering refers to the ELF6 amino acid position.

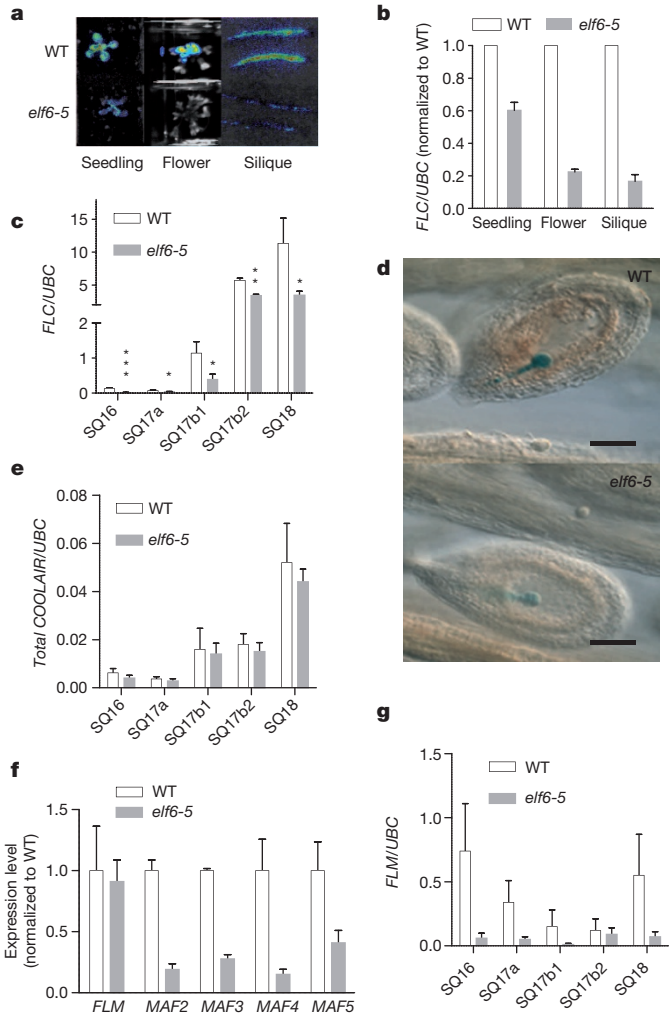

Figure 3 | Characterization of the *elf6-5* resetting mutant. **a**, **b**, *FLC*–luciferase imaging (**a**) and *FLC* qRT–PCR data (**b**) for tissues from the WT and the *elf6-5* mutant in the generation following vernalization. The data are presented as the mean + s.e.m., $n = 6$. Pseudocolour bioluminescent image (**a**) from blue (least intense) to red (most intense). **c**, qRT–PCR data for vernalized WT and *elf6-5* siliques[18]: immediately after fertilization, with petals still attached (SQ16); small and without petals (SQ17a); first (SQ17b1) and last (SQ17b2) mature green siliques; and yellow siliques (SQ18). The data are presented as the mean + s.e.m., $n = 4$; $*P < 0.05$; $**P < 0.01$; $***P < 0.001$ compared with WT. **d**, *FLC*::*GUS* (blue) expression in vernalized WT (top) and *elf6-5* (bottom) early globular embryos. Scale bars, 100 μm. **e**, qRT–PCR shows that *COOLAIR* levels are not affected in *elf6-5* siliques. The data are presented as the mean + s.e.m., $n = 5$. **f**, qRT–PCR data showing that the *MAF2*, *MAF3*, *MAF4* and *MAF5* genes are misregulated in *elf6-5* seedlings in the generation following vernalization. The data are presented as the mean + s.e.m., $n = 3$. **g**, *FLM* has reduced expression in vernalized *elf6-5* siliques. The data are presented as the mean + s.e.m., $n = 3$.

RNAs (siRNAs) produced during seed development[22], including an siRNA homologous to the flanking 3′ region of the *FLC* locus that accumulates preferentially in siliques[23]. Using sensitive northern blot analyses, we did not detect any difference in the amount of these siRNAs between vernalized siliques from *elf6-5* and the parental line (Extended Data Fig. 5). We then asked whether the *elf6-5* allele influenced the expression of other *FLC*-family members[24]. *MAF2*, *MAF3*, *MAF4* and *MAF5* were downregulated in *elf6-5* seedlings and were expressed below the detection level in siliques (Fig. 3f), whereas *FLM* (also known as *MAF1*) expression was unchanged in seedlings but strongly downregulated in *elf6-5* siliques (Fig. 3f, g). The vernalization response in winter-annual *A. thaliana* accessions (containing an active *FRI* allele) depends predominantly on FLC activity[24]; however, in the rapid-cycling Col (*fri*) genotype, all *MAF* genes appear to be direct targets of the polycomb machinery[24,25], indicating that the ELF6-regulatory mechanism that has been elaborated for *FLC* may have more general functions in the *A. thaliana* genome.

Since ELF6 is closely related to the H3K27me3 demethylase REF6, we tested the enzymatic activity of both wild-type and mutant ELF6, by using an *in vivo* histone demethylation assay[16]. We found that transient expression of *A. thaliana* ELF6 resulted in reduced H3K27me2 and H3K27me3 levels in tobacco (*Nicotiniana benthamiana*) leaves (Fig. 4a); no changes were found in the levels of H3K27me1, H3K4me3, H3K9me2 and H3K36me3 (Fig. 4a and Extended Data Fig. 6). These data show that *A. thaliana* ELF6 has histone demethylase activity specific for H3K27me2 and H3K27me3. The *elf6*-5 mutant carries an alanine-to-valine substitution at the C-terminal end of the jumonji C domain. The mutation

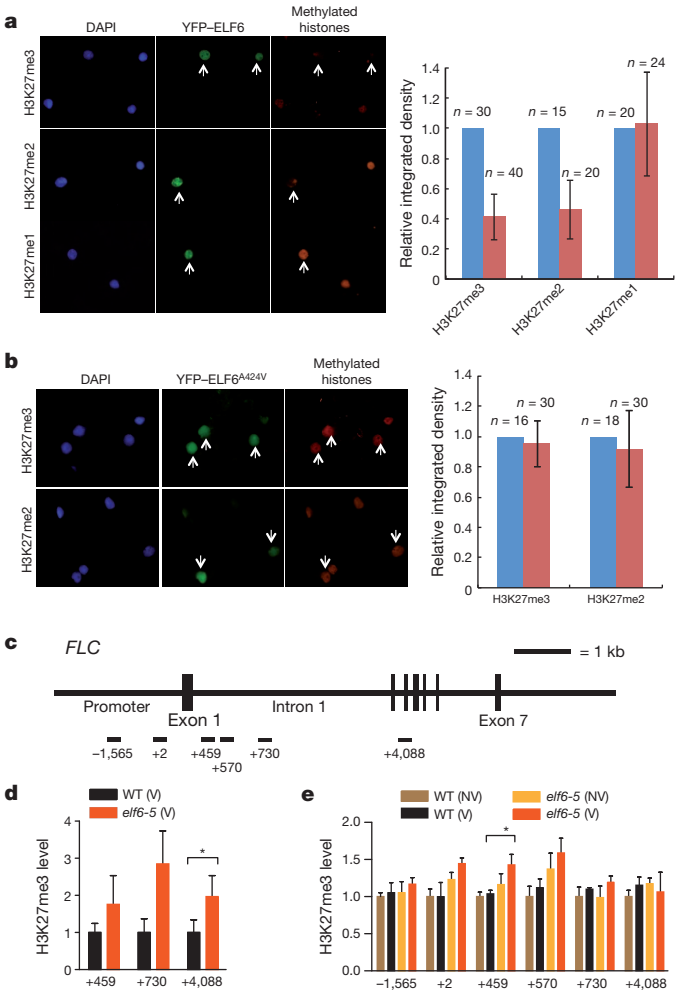

Figure 4 | ELF6 shows H3K27 histone demethylase activity. **a**, **b**, Overexpression of a yellow fluorescent protein (YFP)–ELF6 fusion protein reduces H3K27me3 and H3K27me2 levels but not H3K27me1 levels (**a**, left). Overexpression of YFP–ELF6^{A424V} has no effect on H3K27 methylation (**b**, left). Histone methylation was visualized by immunostaining (red). Nuclei (arrows) from transfected cells were visualized by the YFP signal (green) and stained with DAPI (4′,6-diamidino-2-phenylindole) (blue). The histograms quantify the methylation levels in the nuclei of transfected (red) and non-transfected (blue) cells. The data are presented as the mean ± s.d. **c**, *FLC* regions analysed in ChIP. kb, kilobase. **d**, H3K27me3 levels in *elf6-5* and WT siliques (stage SQ16–SQ17a) from vernalized plants. The data are presented as the mean + s.e.m., $n = 3$. The H3K27me3 level in WT (V) plants is significantly lower than that in *elf6-5* (V) in the *FLC* region +4,088 ($*P < 0.05$). **e**, The H3K27me3 levels in progeny derived from parents that had (V) or had not (NV) been vernalized. The H3K27me3 level in WT (V) plants is significantly lower than that in *elf6-5* (V) in the *FLC* region +459 ($*P < 0.05$). The data are presented as the mean + s.e.m., $n = 3$.

of this highly conserved residue (Fig. 2g) reduced H3K27 demethylase activity in our assay (Fig. 4b). To test whether this reduced activity influenced H3K27me3 levels at the *FLC* locus *in vivo*, we performed chromatin immunoprecipitation (ChIP) experiments. In wild-type Ler (*FRI*) plants, H3K27me3 levels increased by about twofold to fourfold in vernalized seedlings but were reduced to almost non-vernalized levels in vernalized siliques (Extended Data Fig. 7). When the resetting mutant was analysed, we found that the H3K27me3 levels were higher at *FLC* in vernalized young siliques of *elf6-5* mutants than of the parental line (Fig. 4d). ChIP analysis on seedlings of the generation following vernalization also showed increased levels of H3K27me3 over various regions of *FLC* in *elf6-5* mutants (Fig. 4e). These experiments were performed using whole seedlings or siliques; therefore, the data should be interpreted with caution because they are derived from a mixture of tissues. The vernalization-independent increase in H3K27me3 levels in *elf6-5* mutants and the phenotype of the *elf6* loss-of-function mutant make it likely that ELF6 has broader functions than simply resetting H3K27 methylation after vernalization. Nevertheless, all of these data are consistent with the reduced *FLC* expression during embryo development in *elf6-5* mutants involving perturbed H3K27me3 dynamics that affect *FLC* resetting and result in the inheritance of a partially vernalized state.

This effective impairment of the reduction of H3K27me3 levels at *FLC* leads to transgenerational inheritance of a partially vernalized state (Fig. 1a–d). In nature, the consequences of this impairment would be to misalign the developmental program of the plant with respect to the environmental conditions. The sensitivity of *FLC* resetting to the reduced function *elf6-5* allele may indicate that the requirement for H3K27me3 demethylase activity is highest at this post-vernalization stage of development, potentially explaining the differences in phenotype between *elf6-5* and the null allele *elf6-3*. Functional redundancy between the three close homologues REF6, ELF6 and JMJ13 (AT5G46910) may also vary throughout development[16]. It will be interesting to see whether histone variants that are known to change in expression during embryogenesis[26] are also involved in *FLC* resetting. In most eukaryotic genomes, a large proportion of chromatin is decorated with H3K27me3, probably explaining why the erasure of these methyl groups is a tightly controlled event during development and germ cell formation[27]. Further characterization of the *FLC* resetting process should provide greater insight into the molecular mechanism underlying genome reprogramming in eukaryotic organisms.

Online Content Methods, along with any additional Extended Data display items and Source Data, are available in the online version of the paper; references unique to these sections appear only in the online paper.

Received 5 November 2013; accepted 29 July 2014.
Published online 14 September 2014.

1. Feng, S., Jacobsen, S. E. & Reik, W. Epigenetic reprogramming in plant and animal development. *Science* **330,** 622–627 (2010).
2. Paszkowski, J. & Grossniklaus, U. Selected aspects of transgenerational epigenetic inheritance and resetting in plants. *Curr. Opin. Plant Biol.* **14,** 195–203 (2011).
3. Becker, C. *et al.* Spontaneous epigenetic variation in the *Arabidopsis thaliana* methylome. *Nature* **480,** 245–249 (2011).
4. Schmitz, R. J. *et al.* Transgenerational epigenetic instability is a source of novel methylation variants. *Science* **334,** 369–373 (2011).
5. Mansour, A. A. *et al.* The H3K27 demethylase Utx regulates somatic and germ cell epigenetic reprogramming. *Nature* **488,** 409–413 (2012).
6. Canovas, S., Cibelli, J. B. & Ross, P. J. Jumonji domain-containing protein 3 regulates histone 3 lysine 27 methylation during bovine preimplantation development. *Proc. Natl Acad. Sci. USA* **109,** 2400–2405 (2012).
7. Zhao, W. *et al.* Jmjd3 inhibits reprogramming by upregulating expression of INK4a/Arf and targeting PHF20 for ubiquitination. *Cell* **152,** 1037–1050 (2013).
8. Johanson, U. Molecular analysis of *FRIGIDA*, a major determinant of natural variation in *Arabidopsis* flowering time. *Science* **290,** 344–347 (2000).
9. Sheldon, C. C. *et al.* The *FLF MADS* box gene: a repressor of flowering in *Arabidopsis* regulated by vernalization and methylation. *Plant Cell* **11,** 445–458 (1999).
10. Gendall, A. R., Levy, Y. Y., Wilson, A. & Dean, C. The *VERNALIZATION 2* gene mediates the epigenetic regulation of vernalization in *Arabidopsis. Cell* **107,** 525–535 (2001).
11. Song, J., Angel, A., Howard, M. & Dean, C. Vernalization: a cold-induced epigenetic switch. *J. Cell Sci.* **125,** 3723–3731 (2012).
12. De Lucia, F., Crevillen, P., Jones, A. M. E., Greb, T. & Dean, C. A PHD–polycomb repressive complex 2 triggers the epigenetic silencing of *FLC* during vernalization. *Proc. Natl Acad. Sci. USA* **105,** 16831–16836 (2008).
13. Sheldon, C. C. *et al.* Resetting of *FLOWERING LOCUS C* expression after epigenetic repression by vernalization. *Proc. Natl Acad. Sci. USA* **105,** 2214–2219 (2008).
14. Choi, J. *et al.* Resetting and regulation of *FLOWERING LOCUS C* expression during *Arabidopsis* reproductive development. *Plant J.* **57,** 918–931 (2009).
15. Mylne, J., Greb, T., Lister, C. & Dean, C. Epigenetic regulation in the control of flowering. *Cold Spring Harb. Symp. Quant. Biol.* **69,** 457–464 (2004).
16. Lu, F., Cui, X., Zhang, S., Jenuwein, T. & Cao, X. *Arabidopsis* REF6 is a histone H3 lysine 27 demethylase. *Nature Genet.* **43,** 715–719 (2011).
17. Noh, B. *et al.* Divergent roles of a pair of homologous jumonji/zinc-finger-class transcription factor proteins in the regulation of *Arabidopsis* flowering time. *Plant Cell* **16,** 2601–2613 (2004).
18. Roeder, A. H. K. & Yanofsky, M. F. Fruit development in *Arabidopsis. Arabidopsis Book* **4,** e0075 (2006).
19. Bastow, R. *et al.* Vernalization requires epigenetic silencing of *FLC* by histone methylation. *Nature* **427,** 164–167 (2004).
20. Ietswaart, R., Wu, Z. & Dean, C. Flowering time control: another window to the connection between antisense RNA and chromatin. *Trends Genet.* **28,** 445–453 (2012).
21. Slotkin, R. K. *et al.* Epigenetic reprogramming and small RNA silencing of transposable elements in pollen. *Cell* **136,** 461–472 (2009).
22. Mosher, R. A. *et al.* Uniparental expression of PolIV-dependent siRNAs in developing endosperm of *Arabidopsis. Nature* **460,** 283–286 (2009).
23. Swiezewski, S. *et al.* Small RNA-mediated chromatin silencing directed to the 3′ region of the *Arabidopsis* gene encoding the developmental regulator, FLC. *Proc. Natl Acad. Sci. USA* **104,** 3633–3638 (2007).
24. Alexandre, C. M. & Hennig, L. *FLC* or not *FLC*: the other side of vernalization. *J. Exp. Bot.* **59,** 1127–1135 (2008).
25. Kim, D.-H. & Sung, S. Coordination of the vernalization response through a *VIN3* and *FLC* gene family regulatory network in *Arabidopsis. Plant Cell* **25,** 454–469 (2013).
26. Ingouff, M. *et al.* Zygotic resetting of the HISTONE 3 variant repertoire participates in epigenetic reprogramming in *Arabidopsis. Curr. Biol.* **20,** 2137–2143 (2010).
27. Surani, M. A., Hayashi, K. & Hajkova, P. Genetic and epigenetic regulators of pluripotency. *Cell* **128,** 747–762 (2007).

Acknowledgements We thank Dean laboratory members and A. Surani for discussions. The Dean laboratory is supported by the UK Biotechnology and Biological Sciences Research Council grants BB/G009562/1 and BB/C517633/1 and by a European Research Council Advanced Investigator grant (233039 ENVGENE). The Cao laboratory is supported by National Basic Research Program of China grants 2013CB967300 and 2011CB915400 and by the National Natural Science Foundation of China grant 31271363.

Author Contributions P.C. and C.D. designed the research. P.C., H.Y., X. Cui, C.G. and Q.Q. performed experiments. M.T. conducted deep sequencing data analysis. X. Cao contributed new reagents and analytical tools. P.C., H.Y. and C.D. analysed the data and wrote the paper. All authors discussed the results and commented on the manuscript.

Author Information Genomic DNA deep sequencing data for the parental Ler-derived plant and the resetting mutant line have been deposited in the European Nucleotide Archive database under accession number PRJEB6498. Reprints and permissions information is available at www.nature.com/reprints. The authors declare competing financial interests: details are available in the online version of the paper. Readers are welcome to comment on the online version of the paper. Correspondence and requests for materials should be addressed to C.D. (caroline.dean@jic.ac.uk).

METHODS

Plant material and growth conditions. All genotypes except for *elf6-3* (ref. 17) were in a Ler background; an active *FRI JU223* allele and a genomic *FLC*::*LUC* construct were introduced by transformation to generate a vernalization-responsive line in which *in vivo FLC* expression could be monitored by luciferase imaging[15]. Genetic analyses and flowering time experiments were performed with plants sown on soil and grown in controlled environment chambers in long-day conditions (16 h light at 22 °C, 8 h darkness at 20 °C). For vernalization, seeds were pre-grown for 7 days in long-day, warm-growing conditions before being transferred to cold conditions (8 h light and 16 h darkness at 5 °C) for 6 weeks and then returned to warm conditions.

Flowering time. Flowering time was scored as the total leaf number, including rosette and cauline leaves, before the first flower opened. Statistical evaluations were performed with Student's *t*-test.

Reporter gene analysis. The parental Ler (*FRI*) *FLC*::*LUC* line has been described previously[15], and luciferase bioluminescence imaging was detected using a NightOWL CCD photon counting camera (Berthold). Silique valves were opened longitudinally to detect the *FLC*::*LUC* signal from developing embryos. A complementing *pELF6*::*ELF6*::*GUS*::*ELF6-3′*-UTR (3′ untranslated region) construct in an *elf6-1* mutant background was used to monitor *ELF6* expression. *FLC*::*GUS*[19] was introgressed into the resetting mutant, and β-glucuronidase activity was detected in *A. thaliana* embryos. Siliques were longitudinally cut, fixed for 2 h at 20 °C in 90% acetone and washed three times with 50 mM phosphate buffer, pH 7.0, before 24 h incubation at 37 °C in reaction buffer (0.19 mM 5-bromo-4-chloro-3-indolyl-D-glucuronide, 10 mM EDTA, 0.1% Triton X-100, 1 mM potassium ferrocyanide and 1mM potassium ferricyanide in 50 mM phosphate buffer, pH 7.2). Embryos were observed after clearing in Hoyer's medium using a microscope under bright-field Nomarski optics.

RNA expression analysis. For seedlings, RNA analysis seeds were sown on GM media plates, stratified for 2 days and grown in long-day conditions for 11 days. RNA extraction from seedlings, DNase I treatment, cDNA synthesis and qPCR analyses (including the primers for *FLC*, total *COOLAIR* antisense and the *UBC* control gene) were as previously described[28]. The primers for the *MAF*-family genes were as previously described[29,30]. For the study of *FLC* expression in reproductive tissues, each biological replicate was obtained by extracting RNA[31] from the main inflorescence or from three to five siliques from five plants. The expression data are presented as the average of several biological replicates, as indicated in the figure legends. Statistical evaluations were performed with Student's *t*-test.

Illumina sequencing. To identify the resetting mutation, we performed genomic DNA deep sequencing on both the parental Ler-derived plant and the resetting mutant line (European Nucleotide Archive accession number, PRJEB6498). Total genomic DNA was isolated from 2 g inflorescence following a standard procedure. Briefly, inflorescences were ground in liquid nitrogen, and samples were homogenized in extraction buffer (50mM Tris, pH 8, 200 mM NaCl, 2 mM EDTA, 0.5% SDS and 100 mg ml^{-1} proteinase K) and incubated at 37 °C for 30 min. The proteins were removed by phenol–chloroform extraction, and the DNA was precipitated using 2.5 volumes of ethanol in the presence of 3 M sodium acetate, pH 5.

Illumina libraries were prepared using genomic DNA. The Illumina GAIIx sequencing platform was used to generate 76-base paired-end reads for each sample. The alignment program MAQ v0.7.1 (ref. 32) was used, first to map reads from the parental line against the Col-0 (TAIR6) reference sequence. For this parental line, 10,867,014 reads from a total of 14,455,072 were mapped (with 10,265,540 of these in pairs). High confidence SNPs (40,573) identified with the companion maq.pl Perl script were then used, in combination with a list of Ler SNPs (http://signal.salk.edu/atg1001/data/), to edit the original Col-0 reference sequence for use in the subsequent alignment with reads obtained from the mutant line. Reads (58,556,730 from a total of 65,673,308) were aligned with this modified reference sequence, with 55,308,855 of these in pairs, resulting in average 34× coverage. A local instance of the GBrowse genome browser[33] was created and loaded with the modified pseudochromosome sequences and TAIR6 coordinate-based gene model annotations. The mutant SNPs, relative to the Col-0/Ler/parental-adapted reference sequence, were then loaded into the GBrowse MySQL database and made available for visual inspection as an added feature track. By programmatically interrogating the database with a Perl script using Bio::DB::GFF methods, a genome-wide total of 417 ethylmethane sulphonate (EMS) candidates (G/A to C/T in the annotated coding sequence and inferred to induce either non-synonymous codon or donor/acceptor splice site mutations) were then identified for further study.

Genetic complementation. A genomic fragment including the *ELF6* locus was amplified from wild-type Ler genomic DNA using the primers 5′-ATGCCAATC CCAGAAAGTTG-3′ and 5′-AGGAGTCGTTGTCACGCTTA-3′ and was cloned into the pGEM-T vector (Promega). A 7.35-kilobase SacI–KpnI fragment, including full length genomic *ELF6* and its regulatory regions (1.1 kilobases upstream of the start codon and 860 base pairs downstream of the stop codon), was cloned into the pCAMBIA1300 binary vector. Resetting mutant plants were transformed by floral dipping, and hygromycin resistant T_1 plants were isolated. For complementation analyses, parental (Ler (*FRI*) *FLC*::*LUC*), mutant and independent T_2 lines were vernalized, and *FLC*–luciferase activity measured in siliques: eight out of the ten transgenic T_2 lines that were analysed complemented the resetting phenotype. As a control experiment, all T_2 lines were also sown without antibiotic selection, and plants that did not carry the transgene were analysed: all lines without the transgenic *ELF6* construct failed to complement the resetting phenotype.

Sequence alignment. The amino acid sequence alignment of the jumonji C domain of the *A. thaliana* ELF6 (UniProt ID, Q6BDA0), *A. thaliana* REF6 (UniProt ID, Q9STM3), human JMJD3 (UniProt ID, AAH09994) and human UTX (UniProt ID, AAT86073) proteins was performed using the web-based software Multalin tool[34].

Small RNA analysis. Total RNA extraction and northern blot analysis were performed as described previously[23] using seed-specific probes[22].

***In vivo* histone demethylation assay.** The full length genomic coding sequences of wild-type ELF6 or mutant *elf6-5* were cloned into the pEG104 vector[35]. The demethylation assay was carried out as previously described[16]. Briefly, *N. benthamiana* leaves were infiltrated with *Agrobacterium tumefaciens* EHA105 strains carrying a functional wild-type *35S*::*YFP*::*ELF6* or mutant *35S*::YFP::*ELF6*^{A424V}. Nuclei from transfected cells were isolated after 48 h. Immunolabelling of fixed nuclei was performed using histone-methylation-specific antibodies: H3K4me3 (Millipore 07-473, 1:100), H3K9me2 (Millipore 07-441, 1:200), H3K27me3 (Millipore 07-449, 1:100), H3K27me2 (Millipore 07-452, 1:200), H3K27me1 (Millipore 07-448, 1:200) and H3K36me3 (Abcam 9050, 1:100). The modified histones were revealed by Alexa-Fluor-555-conjugated goat anti-rabbit antibody (Invitrogen, 1:200). Transfected cells were revealed by monitoring the YFP signal. After staining, the slides were mounted in VECTAS HIELD Mounting Medium with 4′,6-diamidino-2-phenylindole (DAPI) (Vector Laboratories) and then photographed with an OLYMPUS BX51 fluorescence microscope. Histone methylation levels were quantified by comparing the staining density of a number of transfected *35S*::*YFP*::*ELF6* nuclei with that of the non-transfected nuclei in the same field. Image density was determined using ImageJ software. A negative result in this assay usually corresponded to 80% or less than the total wild-type histone demethylase activity.

ChIP experiments. ChIP experiments were performed using 11-day-old seedlings, using a previously described protocol[12]. For siliques, minor modifications were performed. About 0.5 g tissue was ground in liquid nitrogen, and then the powder was incubated for 10 min at room temperature in extraction buffer containing 1% formaldehyde to fix the tissue. We used anti-H3K27me3 (Millipore, 07-449) and anti-H3 core (Abcam, 1791) antibodies. All ChIP experiments were quantified by qPCR and analysed with previously described primers[36]. The ChIP data are presented as the ratio of H3K27me3 to total H3 normalized to non-vernalized wild-type levels. The ChIP seedling data were also normalized to *STM* H3K27me3 levels[36]. Statistical evaluations were performed using a Student's *t*-test.

Statistical analysis. Statistical evaluations with Student's *t*-test and graphical representation of the data were performed using the Prism software package (GraphPad). The means and s.e.m. are derived from independent biological samples.

28. Crevillén, P., Sonmez, C., Wu, Z. & Dean, C. A gene loop containing the floral repressor *FLC* is disrupted in the early phase of vernalization. *EMBO J.* **32,** 140–148 (2013).
29. Gu, X., Jiang, D., Wang, Y., Bachmair, A. & He, Y. Repression of the floral transition via histone H2B monoubiquitination. *Plant J.* **57,** 522–533 (2009).
30. Jiang, D., Gu, X. & He, Y. Establishment of the winter-annual growth habit via FRIGIDA-mediated histone methylation at *FLOWERING LOCUS C* in *Arabidopsis*. *Plant Cell* **21,** 1733–1746 (2009).
31. Oñate-Sánchez, L. & Vicente-Carbajosa, J. DNA-free RNA isolation protocols for *Arabidopsis thaliana*, including seeds and siliques. *BMC Res. Notes* **1,** 93 (2008).
32. Li, H., Ruan, J. & Durbin, R. Mapping short DNA sequencing reads and calling variants using mapping quality scores. *Genome Res.* **18,** 1851–1858 (2008).
33. Stein, L. D. *et al.* The generic genome browser: a building block for a model organism system database. *Genome Res.* **12,** 1599–1610 (2002).
34. Corpet, F. Multiple sequence alignment with hierarchical clustering. *Nucleic Acids Res.* **16,** 10881–10890 (1988).
35. Earley, K. W. *et al.* Gateway-compatible vectors for plant functional genomics and proteomics. *Plant J.* **45,** 616–629 (2006).
36. Angel, A., Song, J., Dean, C. & Howard, M. A Polycomb-based switch underlying quantitative epigenetic memory. *Nature* **476,** 105–108 (2011).

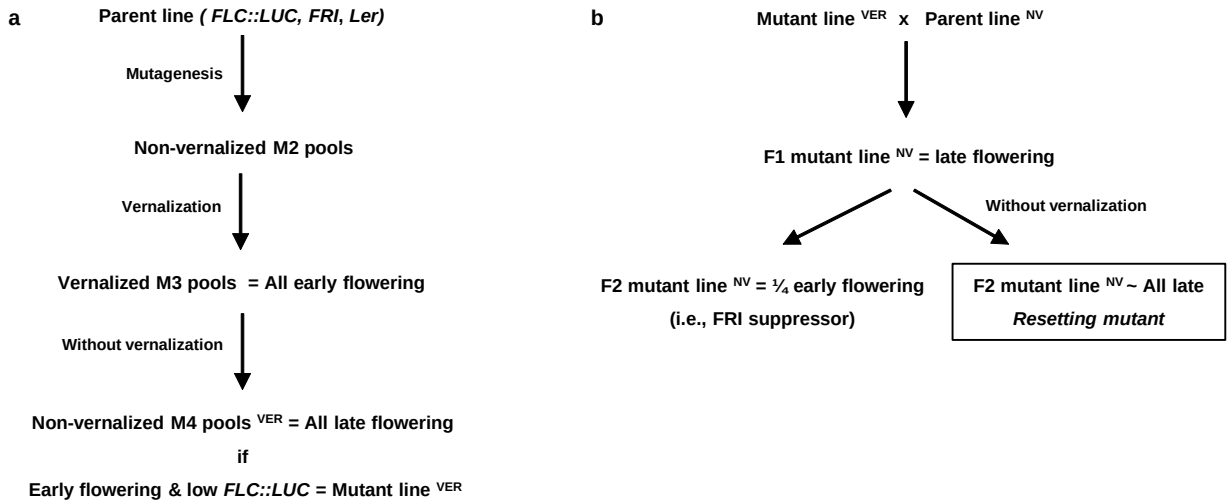

Extended Data Figure 1 | Screening for mutants with impaired epigenetic reprogramming of *FLC*. **a**, We started with a population of ethylmethane sulphonate (EMS)-mutagenized *A. thaliana* Ler plants carrying an *FLC*::*LUC* translational fusion and an active *FRI* transgene. We screened for mutants that were early flowering (as a result of low *FLC* expression) in the generation following vernalization but that did not flower early (and whose *FLC* expression was almost normal) without vernalization. **b**, To discriminate between early flowering and resetting mutants, early flowering M_2 plants were backcrossed to the parental line, and the F_2 phenotype was evaluated without vernalization. Those plants showing no early flowering segregants were considered to be resetting mutants. Superscript characters denote whether the plant was vernalized in the previous generation.

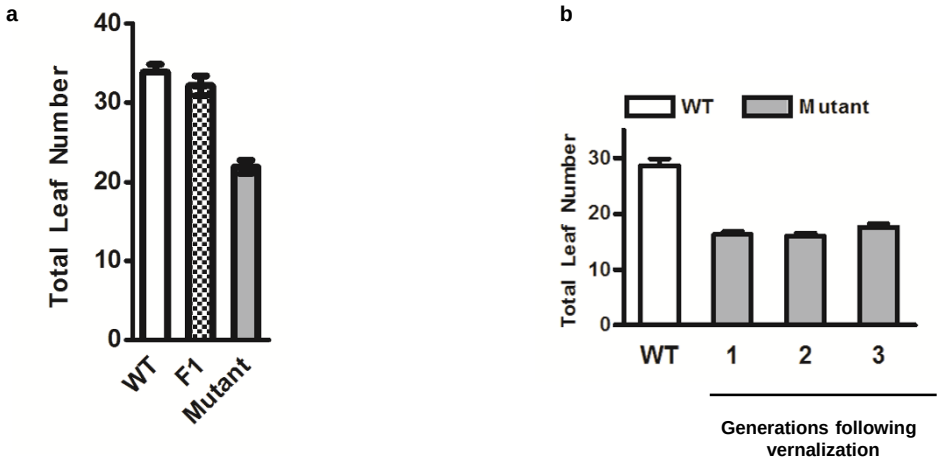

Extended Data Figure 2 | Characterization of the first resetting mutant. **a**, The first resetting mutation was found to be recessive. F_1 plants were generated from a cross between the mutant in the generation following vernalization and the parental wild-type line. Flowering time was assayed as total leaf number under non-vernalized long-day conditions. The data are presented as the mean + s.e.m., $n = 8$. **b**, The earlier flowering time of the mutant in the generation following vernalization was stable for at least three generations without vernalization. The data are presented as the mean + s.e.m., $n = 10$.

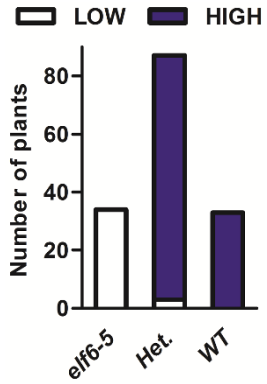

Extended Data Figure 3 | The *elf6-5* SNP is linked to the resetting of *FLC* expression. Histogram showing the relationship between *FLC*::*LUC* levels in the reproductive organs of vernalized plants and the *elf6-5* SNP ($n = 154$).

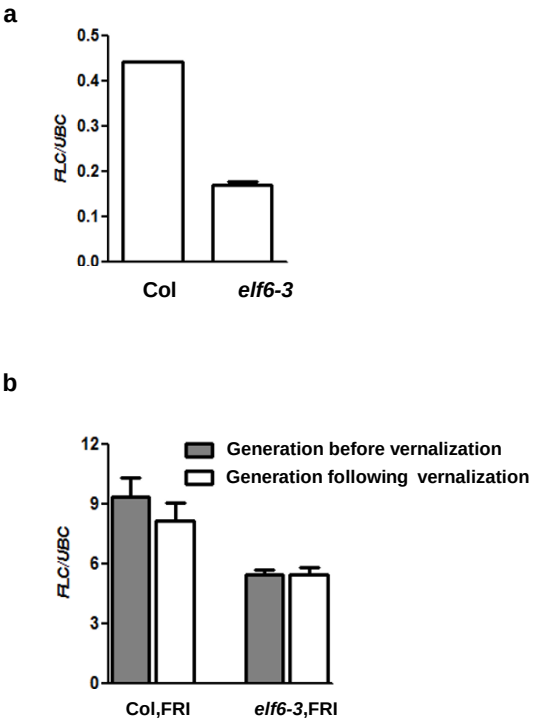

Extended Data Figure 4 | *FLC* expression levels in the null *elf6-3* T-DNA insertion allele. **a**, The *elf6-3* mutant expresses less *FLC* than the Col wild type. **b**, The null *elf6-3* allele suppresses the high *FLC* expression induced by FRI before vernalization. This pre-vernalization phenotype of plants carrying the null allele precludes observation of the role of ELF6 during *FLC* resetting after vernalization. All graphs show 10-day-old non-vernalized seedlings. The data are presented as the mean + s.e.m., $n = 3$.

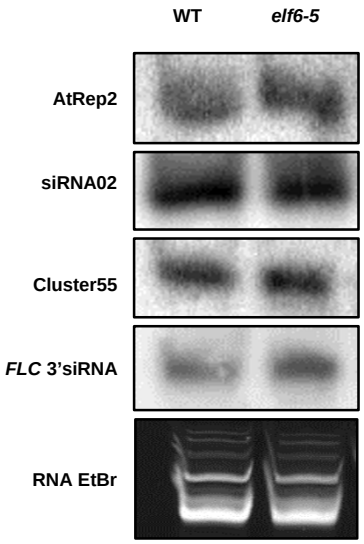

Extended Data Figure 5 | siRNA production in *elf6-5* mutants. The production of specific siRNAs associated with the epigenetic reactivation of transposable elements is not affected in *elf6-5* mutants. Total RNA was extracted from vernalized mature siliques, and the detection of siRNAs was performed as described in Methods.

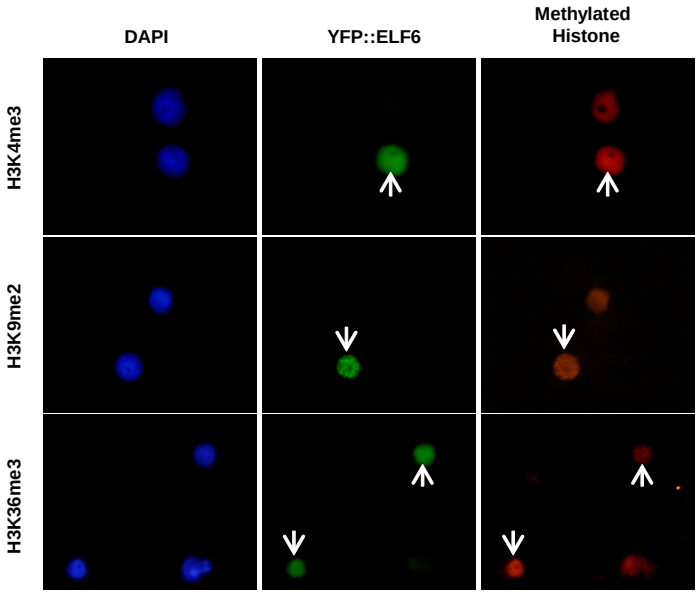

Extended Data Figure 6 | ELF6 has no H3K4me, H3K9me or H3K36me demethylase activity in an *N. benthamiana* transient assay. Overexpression of a yellow fluorescent protein (YFP)–ELF6 fusion protein, using the wild-type ELF6 sequence had no effect on H3K4me3, H3K9me2 or H3K36me3 methylation. Histone methylation was visualized by immunostaining with polyclonal rabbit modification-specific antibodies followed by Alexa-Fluor-555-conjugated goat anti-rabbit antibody (red; right). The nuclei of transfected cells were visualized by the YFP signal (green; centre). Nuclei were stained with DAPI (4′,6-diamidino-2-phenylindole) (blue; left). Arrows indicate the nuclei of transfected cells.

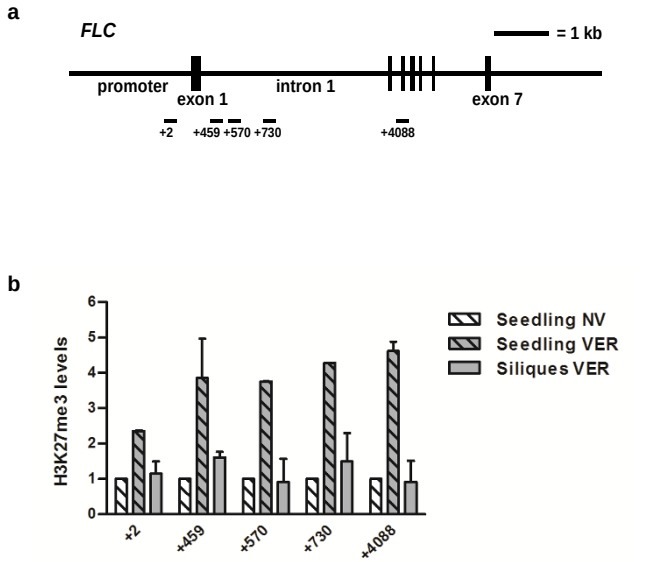

Extended Data Figure 7 | H3K27me3 accumulation at the *FLC* locus. **a**, Schematic representation of the *FLC* locus and the regions analysed in the ChIP assays. **b**, H3K27me3 levels at *FLC* in Ler (*FRI*) seedlings grown without vernalization (seedling NV), 7 days after vernalization (seedling VER) and in siliques from vernalized seedlings (siliques VER). The data are presented as the mean + s.d., $n = 2$.